nature medicine

Hypoxia-inducible factor determines sensitivity to inhibitors of mTOR in kidney cancer

George V Thomas[1], Chris Tran[2], Ingo K Mellinghoff[3–5], Derek S Welsbie[3], Emily Chan[1], Barbara Fueger[4], Johannes Czernin[4] & Charles L Sawyers[2–4,6]

Inhibitors of the kinase mammalian target of rapamycin (mTOR) have shown sporadic activity in cancer trials, leading to confusion about the appropriate clinical setting for their use. Here we show that loss of the Von Hippel-Lindau tumor suppressor gene (*VHL*) sensitizes kidney cancer cells to the mTOR inhibitor CCI-779 *in vitro* and in mouse models. Growth arrest caused by CCI-779 correlates with a block in translation of mRNA encoding hypoxia-inducible factor (*HIF1A*), and is rescued by expression of a VHL-resistant *HIF1A* cDNA lacking the 5′ untranslated region. VHL-deficient tumors show increased uptake of the positron emission tomography (PET) tracer fluorodeoxyglucose (FDG) in an mTOR-dependent manner. Our findings provide preclinical rationale for prospective, biomarker-driven clinical studies of mTOR inhibitors in kidney cancer and suggest that FDG-PET scans may have use as a pharmacodynamic marker in this setting.

The mTOR kinase inhibitor CCI-779 induces objective responses in about 10% and disease stabilization in about 50% of individuals with metastatic renal carcinoma[1]. This finding of selective activity in a subset of individuals raises the possibility that responders share a common molecular phenotype that renders these tumors dependent on mTOR for growth and/or survival. The most common molecular abnormality in renal cell carcinoma is loss of *VHL*, which is found in about 50–70% of sporadic cases[2]. *VHL* encodes an E3 ligase that promotes the ubiquitination of the α-subunits of the hypoxia-inducible transcription factors HIF1, HIF2 and HIF3, leading to their degradation by the proteasome. Consequently, renal carcinomas with mutations in VHL have high steady-state levels of HIF expression. Functional studies show that HIF is sufficient for transformation caused by loss of *VHL*, thereby establishing HIF as the primary oncogenic driver in kidney cancers[3,4].

HIF protein expression is dependent on mTOR in certain cellular contexts[5,6]. The 5′ untranslated regions of mRNAs encoding both HIF-1α and HIF-2α contain 5′ terminal oligopolypyrimidine (TOP) tracts that can regulate translation in response to S6 kinase activation[7]. Translation of mRNAs bearing 5′-TOP sequences is dependent on mTOR because mTOR regulates a kinase cascade, involving S6 kinase and its substrate S6 ribosomal protein, which is required for efficient translation of these messages. This connection between translation of HIF and mTOR raised the possibility that the clinical activity of mTOR inhibitors in a subset of renal cell carcinoma may be explained, in part, by loss of *VHL*.

We evaluated this possibility by constructing isogenic pairs of human renal carcinoma cell lines, differing only in *VHL* expression levels, using stable RNA knockdown by lentiviral transfer of *VHL*-specific shRNA (SN12C and SN12C-*VHL* shRNA; ACHN and ACHN-*VHL* shRNA). As expected, VHL protein levels were reduced and HIF-1α and HIF-2α protein levels were increased in cells stably expressing the knockdown constructs (**Fig. 1a**), whereas vector-only and a control nonspecific shRNA sequence had no effect (**Supplementary Fig. 1** online). Cells containing *VHL*-specific shRNA proliferated more rapidly than their isogenic parental counterparts (**Fig. 1b**), in keeping with previous reports that VHL addback to *VHL*-null cells suppressed growth[8,9]. Protein levels of the HIF target genes, *SLC2A1* (encoding glucose transporter-1), *CA9* (carbonic anhydrase-9) and *VEGF* (vascular endothelial growth factor), were all increased in *VHL* knockdown cells, even under normoxic conditions (**Fig. 1a** and **Supplementary Fig. 2** online[10,11]).

To assess the role of mTOR in proliferation mediated by knockdown of *VHL*, we exposed both isogenic human kidney tumor cell line pairs to the mTOR inhibitor CCI-779. Parental cells were unaffected by 10 nM CCI-779, whereas growth of cells treated with SN12C-*VHL* shRNA (similar results seen with ACHN-CSCG and ACGB-*VHL* cells; data not shown) was reduced by 70% in a dose-dependent fashion. When the isogenic lines were grown as subcutaneous xenografts in SCID mice, stable knockdown of *VHL* again conferred a growth advantage and increased sensitivity to mTOR inhibition even though there was efficient biochemical blockade of mTOR in parental and *VHL* knockdown xenografts (**Fig. 1c–e**). The growth of two renal carcinoma cell lines from the NCI-60 panel with natural mutations in *VHL* (786-0 and A498) was also inhibited by CCI-779 (**Supplementary Fig. 3** online).

In addition to cell-autonomous effects, inhibitors of mTOR have antiangiogenic activity, as growth of endothelial cells is dependent on mTOR in certain settings[12]. Because angiogenesis is a central

[1]Department of Pathology and Laboratory Medicine, [2]Howard Hughes Medical Institute, [3]Department of Medicine, [4]Department of Molecular and Medical Pharmacology, [5]Crump Institute for Molecular Imaging, [6]Department of Urology, David Geffen School of Medicine at UCLA, Los Angeles, California 90095, USA. Correspondence should be addressed to C.L.S. (csawyers@mednet.ucla.edu).

Received 23 August; accepted 4 November; published online 11 December 2005; doi:10.1038/nm1337

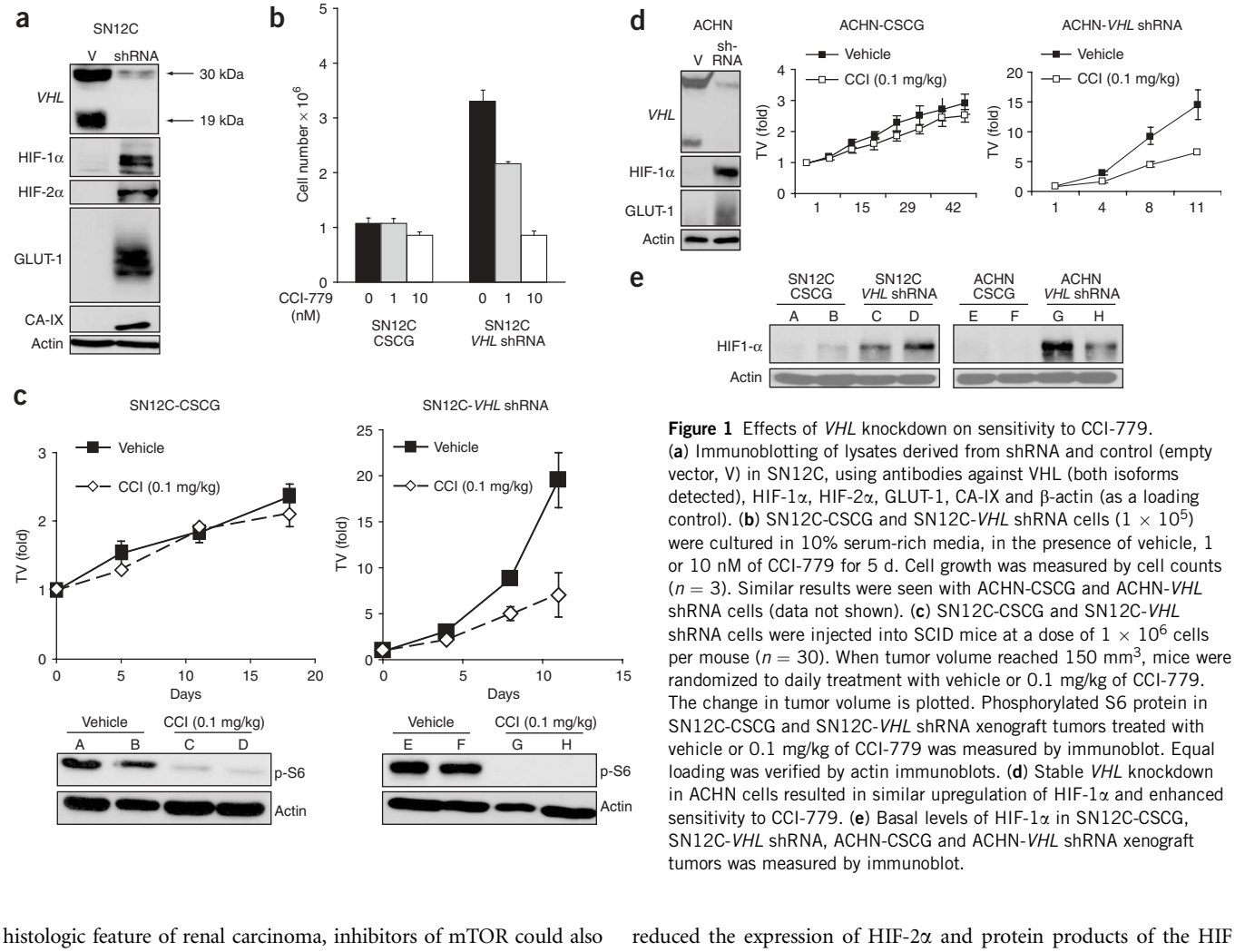

Figure 1 Effects of *VHL* knockdown on sensitivity to CCI-779. (**a**) Immunoblotting of lysates derived from shRNA and control (empty vector, V) in SN12C, using antibodies against VHL (both isoforms detected), HIF-1α, HIF-2α, GLUT-1, CA-IX and β-actin (as a loading control). (**b**) SN12C-CSCG and SN12C-*VHL* shRNA cells (1×10^5) were cultured in 10% serum-rich media, in the presence of vehicle, 1 or 10 nM of CCI-779 for 5 d. Cell growth was measured by cell counts ($n = 3$). Similar results were seen with ACHN-CSCG and ACHN-*VHL* shRNA cells (data not shown). (**c**) SN12C-CSCG and SN12C-*VHL* shRNA cells were injected into SCID mice at a dose of 1×10^6 cells per mouse ($n = 30$). When tumor volume reached 150 mm^3, mice were randomized to daily treatment with vehicle or 0.1 mg/kg of CCI-779. The change in tumor volume is plotted. Phosphorylated S6 protein in SN12C-CSCG and SN12C-*VHL* shRNA xenograft tumors treated with vehicle or 0.1 mg/kg of CCI-779 was measured by immunoblot. Equal loading was verified by actin immunoblots. (**d**) Stable *VHL* knockdown in ACHN cells resulted in similar upregulation of HIF-1α and enhanced sensitivity to CCI-779. (**e**) Basal levels of HIF-1α in SN12C-CSCG, SN12C-*VHL* shRNA, ACHN-CSCG and ACHN-*VHL* shRNA xenograft tumors was measured by immunoblot.

histologic feature of renal carcinoma, inhibitors of mTOR could also impair tumor growth through effects on tumor vasculature. Xenografts from *VHL* knockdown cell lines were more vascular compared to parental tumors ($P < 0.0033$), and treatment with CCI-779 led to a 50% decrease in microvessel density (**Supplementary Fig. 2** online). Given that the proangiogenic gene *VEGF* is a target of HIF, the antiangiogenic properties of CCI-779 might also be a consequence of direct effects of the drug on tumor cells. Indeed, VEGF levels were increased in VHL knockdown cells and reduced by CCI-779 treatment *in vitro* and *in vivo* (**Supplementary Fig. 2** online).

Collectively, these experiments establish that loss of *VHL* sensitizes renal carcinoma cells to growth inhibition by inhibitors of mTOR. One potential mechanism is that translation of mRNA encoding HIF-1α is blocked by inhibitors of mTOR in *VHL*-null cells because of 5′ TOP sequences in the *HIF1A* mRNA[7]. Yet mTOR is inhibited during hypoxic conditions at a time when HIF-1α protein levels are constitutively elevated[13], making it difficult to understand how mTOR might differentially affect expression of HIF-1α in these two contexts. To reconcile this apparent paradox, we examined the effects of CCI-779 on HIF protein levels in *VHL*-intact and *VHL* knockdown cells under both normoxic and hypoxic conditions. As expected[13], HIF protein expression was increased in *VHL*-intact cells by hypoxia, and baseline mTOR activity was reduced compared to normoxia (**Supplementary Fig. 4** online). Expression of HIF-1α and HIF-2α was reduced within 16 h, under both normoxic and hypoxic conditions, after treatment with CCI-779. Similarly, treatment with CCI-779 reduced the expression of HIF-2α and protein products of the HIF target genes *SLC2A1*, *CA9* and *VEGF*. *VEGF* was similarly reduced. These changes correlated precisely with inhibition of mTOR, as measured by reduced phosphorylation of downstream substrates eIF4G and S6 (**Fig. 2a,b**). Therefore, inhibition of mTOR caused by treatment with CCI-779 impairs expression of HIF under both normoxic and hypoxic conditions. A possible explanation for the persistent high levels of HIF during hypoxia despite reduced mTOR activity is that the magnitude of mTOR inhibition induced by hypoxia is insufficient to block expression of HIF (**Supplementary Fig. 4**).

To address the mechanism by which CCI-779 reduces expression of HIF, we examined levels of mRNA encoding HIF and protein stability after treatment with CCI-779. There was no effect on *HIF1A* mRNA (**Fig. 2c**). Potential effects on HIF protein stability were assessed in two ways. The proteasome inhibitor MG-132 did not rescue HIF-1α levels in CCI-779–treated *VHL* knockdown cells, implying that CCI-779 does not induce degradation of HIF (**Fig. 2d**). Furthermore, CCI-779 did not alter the half-life of HIF in *VHL* knockdown cells in cycloheximide-treatment experiments (**Supplementary Fig. 5** online). Therefore, we focused our attention on translation of mRNA encoding HIF-1α through 5′ TOP regulatory sequences. Insertion of native *HIF1A* 5′ TOP sequences into a luciferase reporter conferred CCI-779 sensitivity to reporter protein expression (**Fig. 2e**). We obtained similar findings when we placed the native 5′ TOP sequence upstream of a *HIF1A* cDNA. CCI-779 treatment resulted in a dose-dependent decrease in HIF-1α (by 65%) in the presence of the 5′ TOP sequence,

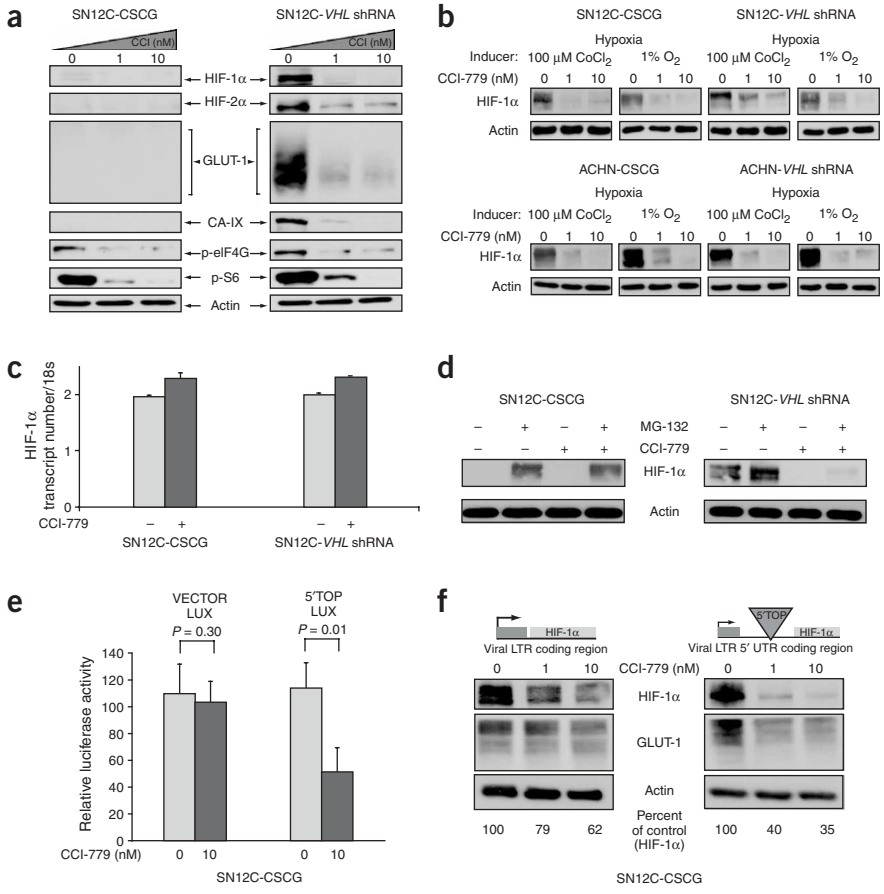

Figure 2 Regulation of HIF expression by mTOR. (**a**) SN12C-CSCG and SN12C-*VHL* shRNA cells were treated with vehicle, 1 nM or 10 nM CCI-779 under normoxic conditions and lysed 24 h later. Lysates were immunoblotted for HIF-1α, HIF-2α, GLUT-1, CA-IX, phosphorylated eIF4G (p-eIF4G), phosphorylated S6 ribosomal protein (p-S6). (**b**) Immunoblot analysis of extracts from isogenic cells pretreated with vehicle, 1 nM or 10 nM CCI-779 for 1 h, followed by exposure to hypoxia ($CoCl_2$ or 1% oxygen) for 16 h. Results were reproduced in at least three independent experiments. (**c**) SN12C-CSCG and SN12C-*VHL* shRNA cells were exposed to either vehicle (–) or 10 nM CCI-779 (+) for 24 h. Total RNA was prepared and quantitative real-time PCR was performed on an ABI Prism 7700 sequence detector (Applied Biosystems). Data are presented as ratio of gene to 18S. (**d**) SN12C-CSCG and SN12C-*VHL* shRNA cells were treated with 10 μM MG-132 for 16 h in the presence or absence of 10 nM CCI-779. (**e**) Stably transformed p-DLN (Vector-LUX, control) or p-DLN-HIF-1α-5′ TOP (5′TOP LUX) cells were plated in triplicate, treated with 10 nM of CCI-779 or vehicle for 24 h and luciferase activity was determined (normalized to total intracellular protein for each sample). Bars and error flags represent mean and s.d. from triplicate samples. (**f**) Expression of HIF-1α was probed by immunoblotting in SN12C–MSCV–5′ TOP–HIF-1α cDNA (right panel) and SN12C–MSCV–HIF-1α cDNA (left panel) after 24 h of vehicle, 1 nM or 10 nM CCI-779. The HIF-1α band intensities were quantified by densitometry, and the numbers below the bottom panel indicate percentage of the vehicle treated control for each dose.

but a 38% decrease in HIF-1α without the 5′ TOP (**Fig. 2f**). Although 5′ TOP sequences clearly account for some of the effects of CCI-779 on levels of HIF-1α, additional sequences in the *HIF1A* cDNA may also have a role.

These experiments establish that CCI-779–mediated growth inhibition of *VHL*-deficient renal carcinoma cell lines correlates with reduced translation of mRNA encoding HIF. Prior work showed that HIF mutants resistant to *VHL*-mediated degradation can rescue *VHL*-mediated tumor suppression. To provide functional evidence that reduced HIF levels are responsible for decreased growth in CCI-779–treated cells, we transduced SN12C *VHL* knockdown cells with *VHL*-resistant *HIF1A* or *HIF2A* mutant cDNAs lacking the 5′ TOP sequences[3,14]. As expected, both HIF mutants (and downstream target genes) were stably expressed in the presence or absence of CCI-779, despite inhibition of mTOR as measured by phosphorylation of eIF4G and S6 (**Fig. 3a**). Notably, both mutants rescued *VHL* knockdown cells from the growth-inhibitory effects of CCI-779 treatment *in vitro* (**Fig. 3b**) and in xenograft experiments (**Fig. 3c**). Therefore, the antiproliferative activity of mTOR inhibitors in *VHL*-null kidney cancer cells is mediated through its effect on translation of mRNA encoding HIF.

These results have important implications for clinical trials of CCI-779 in renal carcinoma as *VHL* status could serve as a biomarker for subject selection. *VHL* data were not collected in the completed phase 2 studies in renal cancer, but estimates of the frequency of mutation in *VHL* can be made from historical data. The anticipated *VHL* mutation rate (~50%) is clearly higher than the objective response rate (~10%) but comparable to the stable disease rate (~50%). As we observed growth arrest (not tumor regression) in our preclinical models, stable disease may be the expected clinical outcome with inhibitors of mTOR in this setting. Alternatively, additional molecular lesions such as expression of Bcl-2 could mitigate the response to inhibition of mTOR[15]. In either case, our findings provide preclinical rationale for correlating *VHL* status with clinical response in future trials, as this might guide future subject selection.

Clinical decision-making would be greatly enhanced by a noninvasive tool for monitoring *VHL* status and response to inhibition of mTOR. Genes of the glycolytic pathway (including *SLC2A1*) were recently linked to activation of HIF in an AKT-driven model of prostate cancer[15]. These findings raise the possibility that HIF-driven tumors might accumulate fluorodeoxyglucose (FDG), the widely used clinical tracer for positron emission tomography (PET). We compared ^{18}F-FDG uptake in both *VHL* knockdown xenograft models relative to parental tumor cells. *VHL* knockdown tumors in both models grown as subcutaneous flank masses reproducibly showed at least a twofold increase in FDG uptake that was reduced to baseline within 24 h with CCI-779. In contrast, paclitaxel had no effect on the FDG-PET uptake, suggesting an mTOR-specific effect (**Fig. 4**). Clinical PET studies in individuals with kidney cancer indicate that a substantial proportion (~50–70%) of these tumors are FDG avid[16], consistent with the expected frequency of *VHL* loss. These results raise the possibility that FDG-PET scanning could be used to noninvasively document inhibition of mTOR in individuals with renal carcinoma before and shortly after initiation of mTOR inhibitor therapy, analogous to the use of

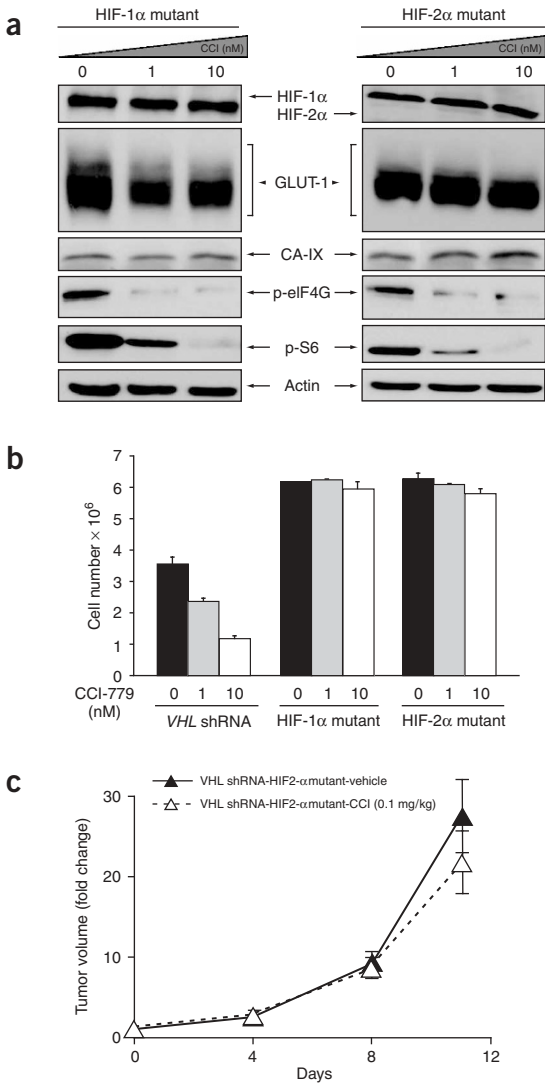

Figure 3 Rescue of CCI-779 growth suppression by HIF-1-α and HIF-2-α prolyl hydroxylase mutants. SN12C-CSCG-*VHL* shRNA cells stably infected with the prolyl hydroxylation defective cDNA mutants p-Babe-puro-HA-HIF-1α (P564A), HIF-2α (P405A; P531A) or backbone vector were treated with CCI-779 or vehicle and harvested 24 h later. (**a**) Lysates were subjected to immunoblotting for HIF-1α, HIF-2α, GLUT-1, CA-IX, p-eIF4G, p-S6 and β-actin as loading control. (**b**) SN12C-*VHL* shRNA, SN12C–*VHL* shRNA–HIF-1α mutant, SN12C–*VHL* shRNA–HIF-2α mutant cells (1×10^5) were cultured in 10% serum-rich media, in the presence of vehicle, 1 or 10 nM of CCI-779 for 5 d. Cell growth was measured by cell counts ($n = 3$). (**c**) SN12C–*VHL* shRNA–HIF-2α mutant cells were injected into SCID mice at a dose of 1×10^6 cells per mouse ($n = 16$). When tumor volume reached 150 mm^3, mice were randomized to daily treatment with vehicle or 0.1 mg/kg of CCI-779. The fold change in tumor volume is plotted.

this scan in individuals with gastrointestinal stromal tumor treated with imatinib[17,18].

Clinical activity has been reported in renal carcinoma using any one of several antiangiogenesis agents that target VEGF (bevacizumab) or its receptor VEGFR (SU11248, Bay 43-9006)[19]. Although inhibitors of mTOR also have antiangiogenic properties[12], our results showing that HIF mutants rescue growth suppression caused by treatment of CCI-779 in mice argue that the antiangiogenic effects of mTOR inhibitors in renal carcinoma are mediated primarily through direct effects on tumor cells. Although the contribution of the microenvironment needs further study[20], this mechanistic understanding provides a rationale for exploring combination therapy using inhibitors of mTOR and the VEGF-VEGFR pathway in renal cancer to block the effects of the activation of the HIF pathway (**Supplementary Fig. 6** online).

Prior work has shown that PI3 kinase–AKT pathway–driven transformation is dependent on mTOR because mTOR is a crucial component of a downstream kinase cascade, consistent with the notion of 'pathway addiction' in tumor cells[21]. Here we provide evidence for kinase dependence through a conceptually distinct mechanism. In renal cell carcinoma caused by loss of *VHL*, the crucial role of mTOR is not transduction of the oncogenic signal downstream of HIF. Rather, translation of HIF mRNA is dependent on mTOR owing to the presence of upstream regulatory signals in its 5′ untranslated region regulated by substrates of mTOR. This model predicts for a highly favorable therapeutic index because decreased translation of mRNA encoding HIF in normal tissues should be inconsequential, as HIF is already rapidly degraded through VHL. A similar mechanism might also be responsible for clinical activity of CCI-779 in mantle cell lymphoma, where the driving oncogenic lesion is presumed to be cyclin D1. Translation of *CCND1* mRNA, which is

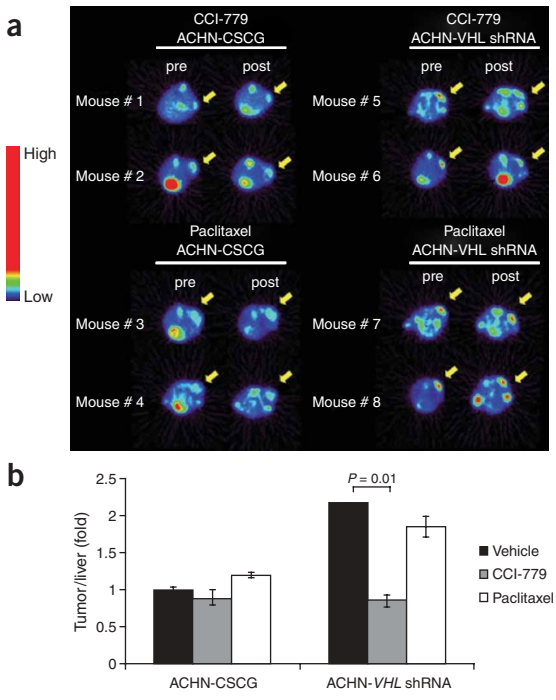

Figure 4 MicroPET imaging shows VHL and mTOR-dependent glucose uptake. (**a**) Representative cross-section ^{18}F-FDG-PET images of SCID mice bearing isogenic ACHN xenograft tumors on the right flank before and after two doses of vehicle, CCI-799 (0.1 mg/kg) or paclitaxel (8 mg/kg). Arrows indicate the location of subcutaneous xenograft tumors (innate increased signal intensity resulting from the intrinsic increase in FDG uptake seen in mouse abdominal brown fat is observed). (**b**) Quantification of FDG uptake (± s.e.m.) in SCID mice bearing either ACHN vector or ACHN-CSCG *VHL* shRNA subcutaneous xenografts. Tumor ^{18}F-FDG uptake was normalized to hepatic ^{18}F-FDG uptake for each mouse and is expressed as fold difference compared to that of the vehicle-treated ACHN-CSCG xenografts; $n = 3$ per group. See Methods for further details.

produced at increased levels as a consequence of the Bcl-1 translocation that defines these tumors, has also been shown to be dependent on mTOR in certain systems[22]. Future clinical trials of mTOR inhibitors might be guided by these distinct conceptual mechanisms of tumor dependence on mTOR.

METHODS

For details, see **Supplementary Methods** online.

DNA constructs and PCR primers. We constructed the pCSUVCG (U6-shRNA-VHL-CMV-GFP) by ligating the *Bam*HI/*Eco*RI digests of pCSCG and the U6-shRNA-VHL PCR product[23]. We performed the U6-shRNA-VHL PCR using a hU6-containing plasmid at an annealing temperature of 60 °C with the primers 5′-GGGGGATCCCAAGGTCGGGCAGGAAGAGGGCCTATTTCC-3′ and 5′-GGGGAATTCAAAAAGACCTGGAGCGGCTGACACTCCTTGAAGTG TCAGCCGCTCCAGGTCGGTGTTTCGTCCTTTCCACAAGATATATAA-3′. We identified the native 5′ untranslated region of *HIF1A* using Genebrowser, which contains previously identified TOP sequences[7]. Using human fetal brain cDNA (Marathon, Invitrogen) as template, we generated a 387-bp fragment containing 268 bp of the 5′ untranslated region and 119 bp of the coding region using the primers 5′-GGGAGATCTGGGGACAGGAGGATCGCC-3′ and 5′-GG GAAGCTCATAAAAAACTTTAGATTC-3′. We subcloned the PCR product into the PCR 2.1 TA cloning vector, verified it by sequencing and subsequently cleaved it with *Bgl*II and ligated it into the *Bgl*II site of the MSCV-puro-*HIF1A* cDNA, to create the *HIF1A* 5′ TOP chimeric gene. We cleaved the *HIF1A* 5′ untranslated region PCR product with *Bgl*II/*Xho*I and subsequently ligated it directionally, 5′ to the renilla luciferase–coding sequence of the pDL-N vector (gift from A. Dasgupta, University of California, Los Angeles). The prolyl hydroxylation–defective mutants of p-Babe-puro-HA-HIF-1α (P564A) and HIF-2α (P405A; P531A) were a gift from W.G. Kaelin (Dana-Farber Cancer Institute).

Immunoblot analysis and luciferase assays. We lysed cells and xenograft tumors in EBC lysis buffer (50 mM Tris, pH 8.0, 120 mM NaCl, 0.5% Nonidet P-40) or high-detergent buffer (2% SDS), respectively, and supplemented them with complete protease and phosphatase inhibitor cocktails (Calbiochem). We resolved protein extracts by SDS-PAGE and transferred them to nitrocellulose membranes. After blocking in Tris-buffered saline (TBS) with 5% nonfat milk, we probed the membranes with following: mouse VHL-specific monoclonal antibody (1:400, Oncogene Research Sciences), mouse HIF-1α–specific monoclonal antibody (1:250, BD Pharmingen), mouse HIF-2α–specific monoclonal antibody (1:500, Novus Biologicals), rabbit GLUT-1–specific polyclonal antibody (1:1,000, Alpha Diagnostic), rabbit CA-IX–specific polyclonal antibody (1:500, Novus Biologicals), rabbit phosphorylated eIF4G-S1108–specific polyclonal antibody (1:1,000, Cell Signaling), rabbit phosphorylated S6 ribosomal protein S235/236–specific polyclonal antibody (1:1,000, Cell Signaling) or mouse β-actin–specific monoclonal antibody (1:5,000, Sigma), diluted in TBS with 4% BSA. We performed densitometric analysis using ImageQuant software.

For hypoxia treatment, we placed cells into a modular hypoxia chamber (Billups Rothenburg) with a regulated environment of 1% O_2, 5% CO_2 and 94% N_2 or cobalt chloride ($CoCl_2$, Sigma) stock solution (100 mM in water) for 16 h.

We transfected SN12C-CSCG with either p-DLN-HIF-5′ TOP (5′ TOP LUX) or p-DLN Vector (Vector LUX) in the presence of Lipofectamine 2000 (Invitrogen) followed by selection in G418. We assayed luciferase activity in triplicate, 24 h after treatment with either 10 nM CCI-779 or vehicle and normalized it to the intracellular protein concentrations within each sample.

***In vitro* and *in vivo* growth experiments.** We maintained SN12C, ACHN, 786-0 and A498 (NCI60, DTP); SN12C-CSCG, ACHN-CSCG, SN12C-CSCG-VHL shRNA and ACHN-CSCG-VHL shRNA in DMEM supplemented with 10% FBS. For *in vitro* experiments, we plated 5×10^4 cells and treated them with a single dose of 1 or 10 nM CCI-779 (gift of J. Gibbons, Wyeth) or vehicle (ethanol). On day 5 after treatment, we trypsinized cells, resuspended them in DMEM with 10% FBS and counted them using the VI-Cell XR automated cell-viability analyzer (Beckmann Coulter). We performed cell counts in triplicate and repeated them on at least three independent occasions. We measured *in vivo* tumorigenicity by subcutaneous injection of 5×10^5 SN12C-CSCG, ACHN-CSCG, SN12C-CSCG-VHL shRNA, ACHN-CSCG-VHL shRNA, SN12C-CSCG-VHL shRNA-pBABE, SN12C-CSCG-VHL shRNA-pBABE-HA-HIF-2α (P405A; P531A) cells in 100 μl of Matrigel (Collaborative Biomedical) into the flanks of SCID mice. We measured tumor size weekly in three dimensions using calipers as previously described[23]. When tumors reached 200 mm^3, we administered 0.1 mg/kg/d CCI-779 or vehicle to all tumors. All mouse experiments were performed in compliance with the guidelines of the Animal Research Committee of the University of California at Los Angeles.

Micro-PET imaging. We synthesized 2-[^{18}F]fluoro-2-deoxy-D-glucose (FDG) using a standard method[24]. We conducted PET scans with the MicroPET Primate 4-ring system (P4; Concorde Microsystems) as previously described. We administered CCI-779 intraperitoneally at a dose of 0.1 mg/kg every 12 h; similarly, we intraperitoneally injected paclitaxel (Sigma) (200 μg; 8 mg/kg) every 12 h. We injected mice intravenously with FDG (7.4 MBq) and imaged them 1 h after tracer injection for 15 min in three independent experiments. For image reconstruction, we first sorted list-mode data into three-dimensional sinograms, followed by Fourier rebinning and two-dimensional filtered back-projection (FBP) reconstruction using a Ramp filter with one-half of the Nyquist frequency as the cut-off frequency. The reconstructed spatial image resolution is ~2.2 mm. For image analysis, we manually placed regions of interest (ROI) around the tumor and the liver on transaxial images. The tumor ROI was defined in the slice with maximum tracer uptake; we placed the liver ROI in the slice with the largest cross-sectional area of the hepatic blood pool. Tracer uptake by the tumors was expressed as the ratio between the maximum intratumoral and mean hepatic counts per pixel. All quantitative values are reported as mean ± s.e.m.

URL. Genebrowser http://genome.ucsc.edu/cgi-bin/hgGateway.

Note: Supplementary information is available on the Nature Medicine website.

ACKNOWLEDGMENTS

This work was supported by grants from the US National Cancer Institute (to G.V.T, I.K.M., C.L.S), the US Department of Defense (to G.V.T., I.K.M., C.L.S.) and Department of Energy (to I.K.M., J.C., C.L.S.). G.V.T. was also supported by grants from the University of California Cancer Research Coordinating Committee, the Stein-Oppenheimer Family Endowment, the Wendy Will Case Foundation and the STOP Cancer Foundation. I.K.M. was also supported by the UCLA Prostate SPORE seed grant. C.L.S. is a Doris Duke Distinguished Clinical Scientist and an Investigator of the Howard Hughes Medical Institute. We thank W.G. Kaelin, G.L. Semenza, J. Gibbons, S. McKnight, R. Bruick, O. Hankinson, A. Dasgupta, R. Strieter, M. Burdick, H. Wu and K. Ellwood-Yen for sharing reagents and advice; members of Sawyers laboratory for helpful discussions and technical assistance; B. Katz for administrative support; M. Costello for graphics support.

COMPETING INTEREST STATEMENT

The authors declare that they have no competing financial interests.

Published online at http://www.nature.com/naturemedicine/
Reprints and permissions information is available online at http://npg.nature.com/reprintsandpermissions/

1. Atkins, M.B. *et al.* Randomized phase II study of multiple dose levels of CCI-779, a novel mammalian target of rapamycin kinase inhibitor, in patients with advanced refractory renal cell carcinoma. *J. Clin. Oncol.* **22**, 909–918 (2004).
2. Kim, W.Y. & Kaelin, W.G. Role of VHL gene mutation in human cancer. *J. Clin. Oncol.* **22**, 4991–5004 (2004).
3. Kondo, K., Klco, J., Nakamura, E., Lechpammer, M. & Kaelin, W.G., Jr. Inhibition of HIF is necessary for tumor suppression by the von Hippel-Lindau protein. *Cancer Cell* **1**, 237–246 (2002).
4. Maranchie, J.K. *et al.* The contribution of VHL substrate binding and HIF1-alpha to the phenotype of VHL loss in renal cell carcinoma. *Cancer Cell* **1**, 247–255 (2002).
5. Hudson, C.C. *et al.* Regulation of hypoxia-inducible factor 1alpha expression and function by the mammalian target of rapamycin. *Mol. Cell. Biol.* **22**, 7004–7014 (2002).
6. Zhong, H. *et al.* Modulation of hypoxia-inducible factor 1alpha expression by the epidermal growth factor/phosphatidylinositol 3-kinase/PTEN/AKT/FRAP pathway in

human prostate cancer cells: implications for tumor angiogenesis and therapeutics. *Cancer Res.* **60**, 1541–1545 (2000).
7. Laughner, E., Taghavi, P., Chiles, K., Mahon, P.C. & Semenza, G.L. HER2 (neu) signaling increases the rate of hypoxia-inducible factor 1alpha (HIF-1alpha) synthesis: novel mechanism for HIF-1-mediated vascular endothelial growth factor expression. *Mol. Cell. Biol.* **21**, 3995–4004 (2001).
8. Chen, F. *et al.* Suppression of growth of renal carcinoma cells by the von Hippel-Lindau tumor suppressor gene. *Cancer Res.* **55**, 4804–4807 (1995).
9. Iliopoulos, O., Ohh, M. & Kaelin, W.G., Jr. pVHL19 is a biologically active product of the von Hippel-Lindau gene arising from internal translation initiation. *Proc. Natl. Acad. Sci. USA* **95**, 11661–11666 (1998).
10. Mandriota, S.J. *et al.* HIF activation identifies early lesions in VHL kidneys. Evidence for site-specific tumor suppressor function in the nephron. *Cancer Cell* **1**, 459–468 (2002).
11. Kaelin, W.G. Proline hydroxylation and gene expression. *Annu. Rev. Biochem.* **74**, 115–128 (2005).
12. Guba, M. *et al.* Rapamycin inhibits primary and metastatic tumor growth by anti-angiogenesis: involvement of vascular endothelial growth factor. *Nat. Med.* **8**, 128–135 (2002).
13. Arsham, A.M., Howell, J.J. & Simon, M.C. A novel hypoxia-inducible factor-independent hypoxic response regulating mammalian target of rapamycin and its targets. *J. Biol. Chem.* **278**, 29655–29660 (2003).
14. Aprelikova, O. *et al.* Regulation of HIF prolyl hydroxylases by hypoxia-inducible factors. *J. Cell. Biochem.* **92**, 491–501 (2004).
15. Majumder, P.K. *et al.* mTOR inhibition reverses Akt-dependent prostate intraepithelial neoplasia through regulation of apoptotic and HIF-1-dependent pathways. *Nat. Med.* **10**, 594–601 (2004).
16. Hain, S.F. & Maisey, M.N. Positron emission tomography for urological tumours. *BJU Int.* **92**, 159–164 (2003).
17. Joensuu, H. Treatment of inoperable gastrointestinal stromal tumor (GIST) with Imatinib (Glivec, Gleevec). *Med. Klin. (Munich)* **97** Suppl. 1, 28–30 (2002).
18. Gayed, I. *et al.* The role of 18F-FDG PET in staging and early prediction of response to therapy of recurrent gastrointestinal stromal tumors. *J. Nucl. Med.* **45**, 17–21 (2004).
19. Ferrara, N., Hillan, K.J., Gerber, H.P. & Novotny, W. Discovery and development of bevacizumab, an anti-VEGF antibody for treating cancer. *Nat. Rev. Drug Discov.* **3**, 391–400 (2004).
20. Blouw, B. *et al.* The hypoxic response of tumors is dependent on their microenvironment. *Cancer Cell* **4**, 133–146 (2003).
21. Weinstein, I.B. Cancer. Addiction to oncogenes—the Achilles heal of cancer. *Science* **297**, 63–64 (2002).
22. Rowinsky, E.K. Targeting the molecular target of rapamycin (mTOR). *Curr. Opin. Oncol.* **16**, 564–575 (2004).
23. Chen, C.D. *et al.* Molecular determinants of resistance to antiandrogen therapy. *Nat. Med.* **10**, 33–39 (2004).
24. Satyamurthy, N., Amarasekera, B., Alvord, C.W., Barrio, J.R. & Phelps, M.E. Tantalum [18O]water target for the production of [18F]fluoride with high reactivity for the preparation of 2-deoxy-2-[18F]fluoro-D-glucose. *Mol. Imaging Biol.* **4**, 65–70 (2002).